A stochastic approach for extended partial blockage detection in viscoelastic pipelines: numerical and laboratory experiments

C. Massari, T.-C. J. Yeh, M. Ferrante, B. Brunone and S. Meniconi

ABSTRACT

Partial blockages in water pipe networks may contribute to large energy dissipation throughout the system and reduce service effectiveness for customers. In this paper, a recently developed stochastic model using transients for detecting partial blockages in water pipelines is tested and numerical and experimental case studies are presented. The model is a stochastic successive linear estimator previously used in groundwater hydrology for detecting the heterogeneity pattern of the subsurface. The model estimates the distribution of diameters within a pipe with partial blockages and quantifies the uncertainty associated with these estimates. Results show that a first good estimate of the extent and size of the blockages can be obtained by a single test generated by the fast closure of a valve.

Key words | partial blockages, pipe system diagnosis, stochastic estimator, transients, viscoelastic

C. Massari (corresponding author)
Research Institute for Geo-Hydrological Protection,
National Research Council CNR,
Via Madonna Alta, 126–06128 Perugia, Italy
E-mail: *christian.massari@irpi.cnr.it*

T.-C. J. Yeh
Department of Hydrology and Water Resources,
The University of Arizona,
John Harshbarger Bldg. 1133E J. E. Rogers Way,
Tucson, AZ 85721, USA

M. Ferrante
B. Brunone
S. Meniconi
Dipartimento di Ingegneria Civile ed Ambientale,
The University of Perugia,
Via Duranti 93–06125 Perugia, Italy

INTRODUCTION

In pressurized pipe, reductions of the pipe's interior cross-sectional area (hereafter referred to as partial blockages) may be due to, for example, deposition of sediments and fouling processes. They may noticeably reduce the performance of systems as well as increase management costs. Indeed, partial blockages cause a reduction of the carrying capacity in gravity systems and an energy consumption increase in pumping systems. Moreover, they also serve as a food source for bacteria, creating a hospitable environment for microbial growth and/or they may cause water quality deterioration (Boulos *et al.* 2006). It is worth noting that, as opposed to anomalies that give rise to an evident symptom, i.e. the external flow of leaks, partial blockages can cause less evident effects. Therefore, the need to develop more reliable techniques for locating and sizing partial blockages is more urgent.

In the last couple of decades, reflectometry has been shown to be an accurate method for the diagnosis of such features in pipelines. To this end, both acoustic (Papadopoulou *et al.* 2008) and pressure waves can be used.

In this paper, attention is focused on transient test-based techniques within which pressure waves explore the pipe and allow anomalies to be detected since a reflected pressure wave is originated at each of them (e.g. a partial blockage, a leak, a partially closed in-line valve, local wall stiffness drop, etc.). By analysing the variations caused by the anomalies in pressure time-history (hereafter referred to as the pressure signal) at some measurement sections, their location and size can be evaluated. Moreover, since the characteristics of the pressure signal are strongly related to those of the anomaly, it is possible to easily diagnose the fault. For example, it is possible to distinguish between discrete and extended partial blockages due to partially closed in-line valves and short branches of pipe with a smaller interior diameter, respectively (Brunone *et al.* 2008).

According to the literature, the analysis of the pressure signal can be executed in both the frequency (Wang *et al.* 2005; Mohapatra *et al.* 2006a, b; Lee *et al.* 2008, 2013; Sattar *et al.* 2008; Duan *et al.* 2012a, 2013, 2014a, b; Tuck *et al.* 2013) and time-domain (Contractor 1965; Meniconi

et al. 2011a, b, 2012a, b); more recently, a coupled approach has been proposed (Meniconi *et al.* 2013). Indeed quite reliable results have been achieved not only in laboratory pipes, but also in real pipe systems (Stephens *et al.* 2004; Ferrante *et al.* 2009a; Meniconi *et al.* 2010). An alternative approach, which is also the first to have been proposed, at least for leak detection (Liggett & Chen 1994), is one based on the inverse transient analysis (ITA). According to this approach, the pipe diagnosis is obtained solving the equations governing transients and then comparing the numerical and experimental results. Within such an approach, a proper modeling of the most important phenomena, such as unsteady friction and, in the case of polymeric pipes, viscoelasticity, is needed (Duan *et al.* 2010, 2012b). When the ITA approach is followed, the unknowns are the parameters of the system; when the aim of such a procedure is pipe diagnosis, then the characteristics of the partial blockages (location, size, and extent) are the unknowns of the problem. If, as in most literature, the governing equations are solved in a deterministic framework, a unique value is obtained for the unknown quantities and no information is given about its reliability. Moreover, the effect on the precision of the estimation of the unknowns due to the use of additional data cannot be determined quantitatively. As an example, it is not possible to properly evaluate the effect of the number of the executed tests and their duration on accuracy in the determination of the unknowns.

In this paper, an extension of Massari *et al.* (2014b), the stochastic successive linear estimator (SLE) proposed in groundwater hydrology (Yeh *et al.* 1996) is used to infer the presence of extended partial blockages in viscoelastic pipes. The algorithm relies on the use of the cokriging estimation technique (Yeh & Zhang 1996) which is based on the assumption of (i) a linear relationship between the quantities involved on the estimate and (ii) a Gaussian stochastic process (Kitanidis & Vomvoris 1983). However, when dealing with non-linear systems, the assumption of linearity is an important limitation of the method (Yeh *et al.* 1996). Such a limitation has been overcome by introducing the SLE approach that considers the successive improvements of the estimates by solving the governing equations and updating the covariance and cross-covariance matrices of the parameters and unknowns' fields in an iterative

manner (Yeh *et al.* 1996; Vargas-Guzmán & Yeh 2002; Zhu & Yeh 2005).

The approach of detecting partial blockages by SLE significantly differs from what can be found in the literature. In fact, the characteristics of the partial blockage are calculated by estimating the distribution of the diameters along the pipe. That is, the unknown of the inverse problem is the function $D(x)$, with D and x being the internal diameter and the location along the pipe, respectively. The algorithm casts the inverse problem of the diagnosis in the probabilistic framework. In fact, it uses a pressure signal recorded during a transient test to (i) estimate the diameter distribution resulting from the formation of a partial blockage and (ii) provide the uncertainty associated with these estimates.

In this paper, four tests are executed. The first two tests are numerical (num): test 1 is used to check the performance of the algorithm when dealing with data affected by noise; test 2 deals with data affected by model structure errors. The last two tests are experimental (laboratory): tests 3 and 4 show the behavior of SLE when laboratory data are considered. Although several approximations are made, the considered tests show that SLE provides a cheap technique to detect extended blockages and to estimate their characteristics.

MATERIALS AND METHODS

The aim of this section is to illustrate the laboratory setup, the forward one-dimensional (1-D) numerical model, and SLE.

Laboratory setup

Experiments were carried out at the Water Engineering Laboratory of the University of Perugia, Italy, in high density polyethylene pipes (Figure 1) supplied by an upstream reservoir (R). The partial blockage (BL, pipe #2) is simulated by means of a small-bore pipe with $D_2 = 38.30$ mm, nominal diameter DN50, wall thickness, $e_2 = 3.9$ mm, and two different lengths, $L_2 = 3.56$ and 6.60 m. The pipe upstream (pipe #1), that links the supply reservoir to the partial blockage, has a length $L_1 = 62.23$ m whereas the downstream pipe (pipe #3), that links the partial blockage to the end maneuver
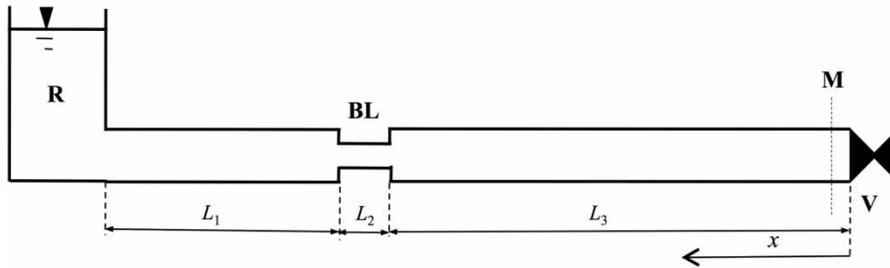
Figure 1 | Sketch of the experimental and numerical setup (R = supply reservoir, BL = extended partial blockage, V = maneuver valve, M = measurement section, and x = location along the pipe).

valve (V), has a length $L_3 = 110.44$ m; such pipes have $D_1 = D_3 = 93.3$ mm, DN110, and $e_1 = e_3 = 8.1$ mm. The same pipe system has been considered for the numerical tests.

Transients were generated by the complete and fast closure of the end valve (V). The pressure signal, h, at a section immediately upstream of V (section M) and the pre-transient discharge, Q_0, were measured by a piezo-resistive transducer and an electromagnetic flow-meter, respectively. The pressure signals were de-noised by means of a wavelet filter (Ferrante *et al.* 2007, 2009b). In Figure 2(a) and 2(b) the pressure signals acquired during tests 3 and 4 – with a frequency acquisition of 2,000 and 1,024 Hz, respectively – are reported, with t being the time. For test 3, the maneuver duration, T, is equal to 0.08 s and $Q_0 = 2.4$ L/s, whereas for test 4 it is $T = 0.065$ s and $Q_0 = 2.7$ L/s (Table 1).
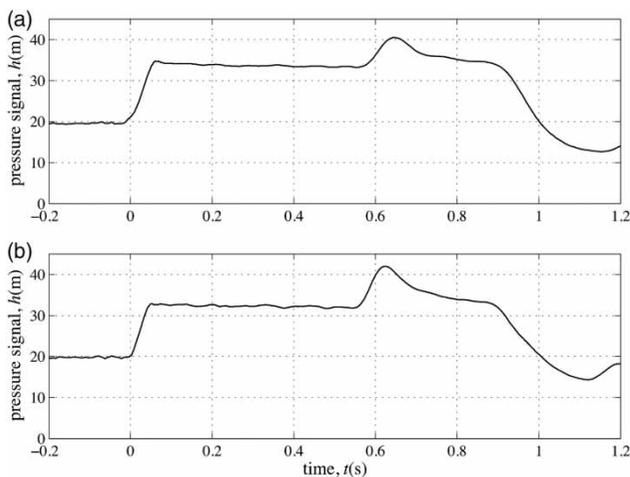

Figure 2 | Pressure signals at section M immediately upstream of V during (a) test 3 and (b) test 4.

Governing equations

The 1-D unsteady flow of a compressible liquid in a viscoelastic pipe can be simulated by means of the following equations (Covas *et al.* 2005; Soares *et al.* 2008; Keramat *et al.* 2012; Meniconi *et al.* 2014; Pezzinga *et al.* 2014):

$$\frac{\partial h}{\partial t} + \frac{a_{\text{el}}^2}{gA}\frac{\partial Q}{\partial x} + \frac{2a_{\text{el}}^2}{gA}\frac{d\epsilon_r}{dx} = 0 \quad \frac{\partial h}{\partial x} + \frac{Q}{(gA)^2}\frac{\partial Q}{\partial x} + \frac{1}{gA}\frac{dQ}{dt} + J = 0 \tag{1}$$

where A = pipe cross-sectional area, g = gravitational acceleration, a_{el} = elastic pressure wave speed, ϵ_r = retarded strain, and J = friction term. In Equation (1), ϵ_r takes into account the effect of the rheological behavior due to the retarded increasing deformation occurring during the application of a constant stress in viscoelastic materials. In fact, differently from elastic materials, when a certain instantaneous circumferential stress, σ, is applied to a viscoelastic material, the resulting total strain, ϵ, is given by the summation of two components the instantaneous elastic one, ϵ_{el}, and ϵ_r. To simulate the behavior of viscoelastic materials, a single element Kelvin–Voigt model is assumed (Franke & Seyler 1983). This element consists of a viscous damper and elastic spring connected in parallel and is jointed to a simple elastic spring in series. Since a single element Kelvin–Voigt model is used, in Equation (1) ϵ_r is given by the following relationship:

$$\sigma = E_r\epsilon_r + \frac{E_r}{T_r}\frac{d\epsilon_r}{dt} \tag{2}$$

where $\sigma = \psi pD/2e$, with ψ = dimensionless parameter that takes into account pipe size and constraints, p = internal

Table 1 | Summary of numerical (num) and laboratory (lab) tests

Test	L_1 (m)	L_2 (m)	L_3 (m)	D_1 (mm)	D_2 (mm)	Q_0 (L/s)	T (s)	VE	UF	NOISE	Num/lab
1a	130	8	22	93.30	40.00	2.4	0.0173	Yes	No	No	Num
1b										Yes	
2	62.23	3.56	110.44	93.30	38.30	2.4	0.08	Yes	Yes	No	Num
3	62.23	3.56	110.44	93.30	38.30	2.4	0.08	Yes	Yes	Yes	Lab
4	62.23	3.56	110.44	93.30	38.30	2.7	0.065	Yes	Yes	Yes	Lab

pressure, E_r = dynamic modulus of elasticity, and T_r = retardation time of the viscous damper of the Kelvin–Voigt element. The instantaneous elastic strain, ϵ_{el}, of the spring is given by

$$\epsilon_{el} = \frac{\sigma}{E_{el}} \tag{3}$$

where Young's modulus of elasticity, E_{el}, is linked to a_{el} by:

$$a_{el} = \sqrt{\frac{k/\rho}{1 + \psi(kD/eE_{el})}} \tag{4}$$

with k = bulk modulus of elasticity and ρ = fluid density.

At any instant, in Equation (1), the total friction term J is regarded as the sum of two components

$$J = J_s + J_u \tag{5}$$

where J_s is the quasi steady-state value based on the instantaneous mean flow velocity

$$J_s = \lambda \frac{Q|Q|}{2gDA^2} \tag{6}$$

with λ = friction factor, and the additional contribution due to unsteadiness, J_u, is evaluated by an instantaneous acceleration-based model (Brunone et al. 1995; Pezzinga 2000; Bergant et al. 2001; Brunone & Golia 2008):

$$J_u = \frac{k_u}{2gA}\left(\frac{\partial Q}{\partial t} + a_{el}\text{sign}(Q)\left|\frac{\partial Q}{\partial s}\right|\right) \tag{7}$$

in which k_u = unsteady friction coefficient and sign(Q) = +1 for $Q \geq 0$ or −1 for $Q < 0$; for all pipes λ is evaluated

properly by means of the Blasius formula (Brunone & Berni 2010).

The calibration procedure followed for evaluating the viscoelastic (E_{el}, ψ, E_r, and T_r) and unsteady friction (k_u) parameters is described in detail in Meniconi et al. (2012a, b, 2013, 2014). The following values of such parameters allow transients to be simulated properly: $E_{el} = 2.2 \ 10^9$ Pa, $\psi = 1.2535$, $E_r = 8.5 \ 10^9$ Pa, $T_r = 0.13$ s, and $k_u = 0.0015$, for pipes #1 and #3 (DN110); $E_{el} = 2.62 \ 10^9$ Pa, $\psi = 1.2945$, $E_r = 15 \ 10^9$ Pa, $T_r = 0.08$ s, and $k_u = 0.02$, for pipe #2 (DN50).

The head and discharge values are calculated by the method of characteristics, leading to a matrix form similar to the one proposed by Liggett & Chen (1994)

$$\{u\} = [M]^{-1}\{R\} \tag{8}$$

where $[M]$ is the coefficient matrix, $u = \{h \ Q \ \epsilon_r\}$ is the solution vector of the heads, discharges and the strains, and $\{R\}$ is the vector associated with the boundary conditions. Equation (8) defines a non-linear system of equations and must be solved at each time step.

SLE

In this study, SLE is used for estimating the diameter distribution of the pipe following the method used in Massari et al. (2013a, b). The algorithm assumes the pipe diameter as a stationary stochastic process with a constant unconditional mean $Y_d = \text{E}[\ln D]$ and unconditional log-perturbation $d(x)$, i.e. $\ln D(x) = Y_d + d(x)$, (E[·] denotes the expected value operator). The corresponding pressure signal, h, is given by $h(x) = \Phi(x) + \phi(x)$ where $\Phi(x) = \text{E}[h(x)]$ is the mean of $h(x)$ and $\phi(x)$ the unconditional head

perturbation. A first estimate of $d(x)$ is obtained by a linear combination of the weighted observed values of d and ϕ:

$$\hat{d}(x_0) = \sum_{k=1}^{N_\phi} \beta_{dk}\phi(x_k) \tag{9}$$

where $\hat{d}(x_0)$ is defined as the cokriged value at location x_0 and N_ϕ is the number of observed heads. The weights β_{dk} are evaluated by requiring that the estimation expressed by Equation (9) has a minimum variance. The latter leads to a linear system of equations in terms of the covariance matrix $C_{\phi\phi}$, and the cross-covariance matrix, $C_{\phi d}$:

$$\sum_{pk=1}^{N_\phi} \beta_{dk}C_{\phi\phi}(x_k, x_{pk}) = C_{\phi d}(x_k, x_0) \tag{10}$$

The covariance $C_{\phi\phi}$ and the cross-covariance $C_{\phi d}$ in Equation (10) are derived by the first-order numerical approximation (Dettinger & Wilson 1981). The values of the diameter are then obtained by $D(x_0) = \exp[Y_d(x_0) + d(x_0)]$. SLE also allows for evaluating the uncertainties associated with the estimates of the conditional covariance:

$$\varepsilon_{dd}^{(1)}(x_0, x_0) = C_{dd}(x_0, x_0) - \sum_{k=1}^{N_\phi} \beta_{dk}C_{d\phi}(x_k, x_0) \tag{11}$$

where C_{dd} = covariance matrix of diameters.

To account for the non-linear relationship between d and h not embedded in the cokriging, SLE is used. That is

$$\hat{Y}_d^{(r+1)}(x_0) = \hat{Y}_d^{(r)}(x_0) + \sum_{j=1}^{N_\phi} \omega_{j0}^d[h_j*(x_j) - h_j^{(r)}(x_j)] \tag{12}$$

where ω_{j0}^d are weighting coefficients to estimate the diameter at location x_0 with respect to the head measurements at location x_j, and r is the iteration index. $\hat{Y}_d(x_0)$ is the estimate of the conditional mean of $\ln D(x_0)$, h_j* is the observed head at location x_j, and $h_j^{(r)}$ is the simulated head at the same location based on the estimates at the rth step. The weights ω_{j0}^d are selected by requiring the minimum variance of Equation (11).

The conditional covariances are evaluated according to

$$\epsilon_{dd}^{(r+1)}(x_0, x_k) = \varepsilon_{dd}^{(r)}(x_0, x_k) - \sum_{k=1}^{N_\phi} \omega_{i0}^{d(r)}\varepsilon_{d\phi}^{(r)}(x_i, x_k) \tag{13}$$

which gives the accuracy of the estimate $\epsilon_{dd}(x_0, x_0)$ at each iteration: the smaller $\epsilon_{dd}(x_0, x_0)$, the more accurate the estimate. After obtaining the value of $Y_d(x_0)$, the governing equations are solved again with the new value of $Y_d(x_0)$ leading to new head data $\{h\}$; then, appropriate norms of the parameters and of the heads are evaluated. If the norms are smaller than the prescribed tolerances, the iteration stops, otherwise Equations (10) and (12) are solved again. For further details of the algorithm the reader is referred to Yeh *et al.* (1996) and Massari *et al.* (2013a, b, 2014a, b).

NUMERICAL AND LABORATORY TESTS

In Table 1 a summary of the executed numerical and laboratory tests is reported: the values of pipe lengths, L_i, and diameters, D_i, the pre-transient discharge, Q_0, the closure maneuver duration, T, and whether viscoelasticity (VE), unsteady friction (UF), and noise (NOISE) are taken into account for numerical (num) tests.

The numerical pressure signals are simulated by the forward model for 1 s at a rate of 185 and 2,000 Hz for tests 1 and 2, respectively. Test 1 (Figure 3) has been executed to preliminarily check the effect of the noise on the reliability of the approach. That is, the results of the procedure applied to a 'perfect' (i.e. without noise) signal (test 1a) are compared with those obtained with noisy data (test 1b). The white noise has been generated by assuming a Gaussian distribution with zero mean and a standard deviation equal to ±0.3% of the maximum recorded pressure value in order to resemble the actual signals recorded by standard pressure transducers.

The aim of test 2 (Figure 4), which simulates numerically the experimental test 3, is to check the performance of the partial blockage estimation when UF is considered
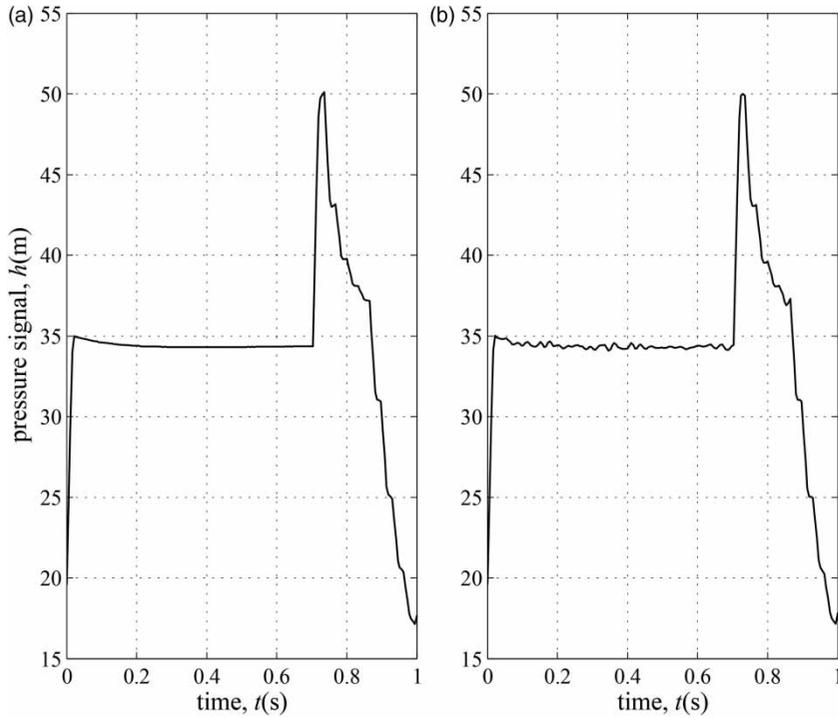
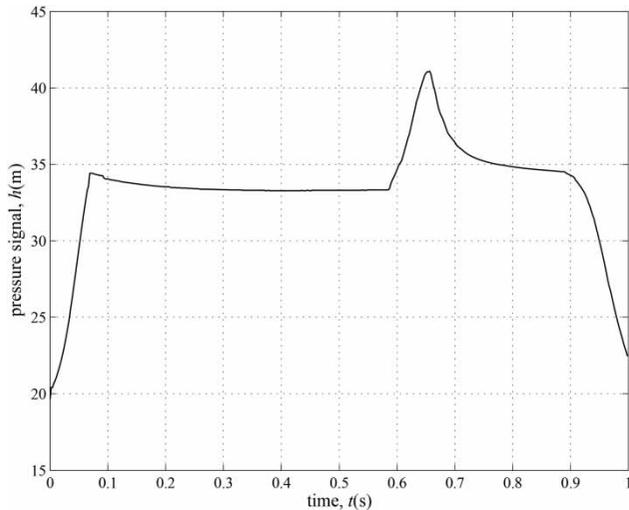**Figure 3** │ Test 1: pressure signal (a) without noise and (b) with additive white noise.

Figure 4 │ Test 2: numerical pressure signal that simulates the experimental pressure signal of Figure 1(a) (test 3).

and different wave speeds and viscoelastic parameters are chosen for the pipes of the system. Finally, experimental tests 3 and 4 (Figure 2(a) and 2(b), respectively) are used to check the behavior of SLE with true data.

RESULTS AND DISCUSSION

Test 1

In this case, the inverse problem is free of model structure errors – e.g. those due to UF, VE, minor losses at the section changes, wave speed variations along the pipe – since the same forward model is used to generate them. The pipe system is parametrized by considering 80 blocks with a spatial resolution $\Delta x = 2$ m: pipe #1 is divided in 65 blocks whereas pipe #2 in 4 and pipe #3 in 11 blocks.

Figure 5 compares the true and the estimated diameters along x for test 1 without noise (Figure 5(a)) and with additive noise (Figure 5(b)) while Figure 6 gives the relative percentage errors along x defined as:

$$\Delta_f = 100|f_{\text{true}} - f_{\text{est}}|/f_{\text{true}} \tag{14}$$

with $f_{\text{true}} =$ true value of the quantity f, $f_{\text{est}} =$ estimated value of the quantity f (in this case $f = D$). SLE catches the presence of pipe #2 by inferring its smaller diameter at right

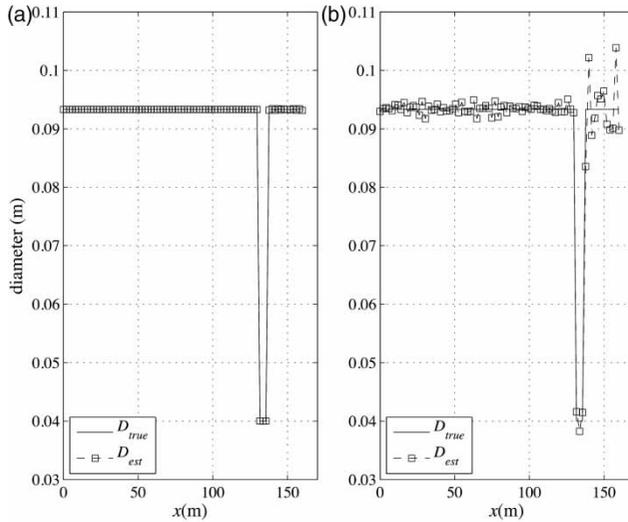**Figure 5** | Test 1: estimated and true diameters along x (a) without noise and (b) with additive white noise.
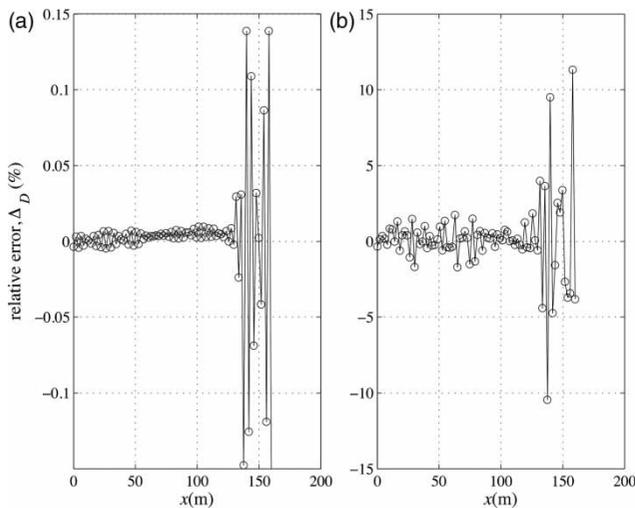

Figure 6 | Test 1: relative errors between estimated and true diameters along x (a) without noise and (b) with noise.

locations. However, the results show that the estimation is greatly affected by data measurement errors giving relative errors for test 1b of approximately one order of magnitude larger than those of test 1a.

Table 2 shows the statistical analysis of the relative errors of Figure 6. The mean and the standard deviation of Δ_D are about two orders of magnitude smaller for test 1a (without noise) with respect to test 1b (with white noise). Furthermore, in terms of the mean squared error (MSE), test 1a provides a much smaller value of MSE = 4.81e-5 $\times 10^{-5}$ m compared to the value of MSE for test 1b (2.80×10^{-2} m).

Table 2 | Statistical analysis of relative percentage errors obtained for test 1

Test	Mean of Δ_D (m)	Standard deviation of Δ_D (m)	Max of Δ_D (%)	MSE (m)
1a	6.25×10^{-7}	4.0×10^{-5}	0.16	4.81×10^{-5}
1b	1.04×10^{-4}	2.3×10^{-2}	11.32	2.80×10^{-2}

Test 2

In the inverse problem, the viscoelastic parameters and the unsteady friction are considered constant for all pipes and equal to those evaluated experimentally for pipes #1 and #3. The pipe is discretized into 200 blocks, and then 200 diameter values have to be estimated, leading to a spatial resolution $\Delta x = 0.8425$ m and a time step $\Delta t = 0.0022$ s. As an initial guess for the estimation procedure, the pipe is supposed to be of a constant diameter equal to $D_1 = 0.0933$ m. The pressure signal is downsampled by means of a linear interpolation, obtaining 448 head values. According to such parametrization, the estimation does not enable the exact detection of blockage location and extent. Such errors can be reduced if a higher resolution is chosen (i.e. by dividing the pipe with a larger number of blocks). However, such a resolution has been chosen in the light of the available computational resources. SLE converges in 48 iterations with a computational time of 48 hours (CPU Intel Core Duo 2.16 Ghz, RAM 4 Gb).

Figure 7(a) compares the true and the estimated diameters along x obtained by SLE; in Figure 7(b) the relative
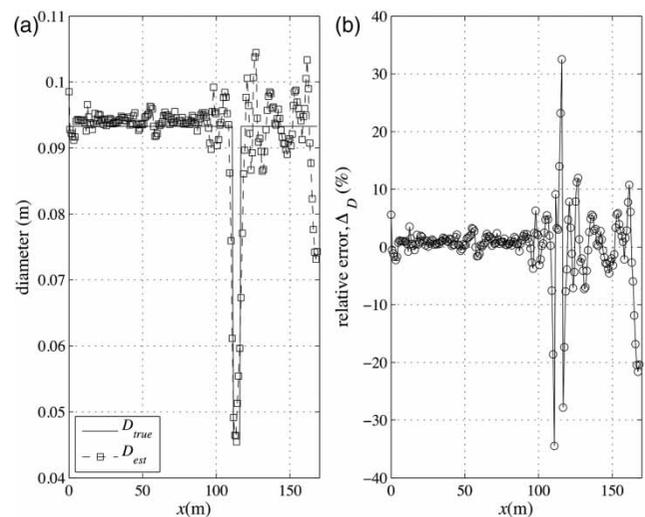

Figure 7 | Test 2: (a) estimated vs. true diameters along the pipe and (b) relative percentage errors Δ_D.
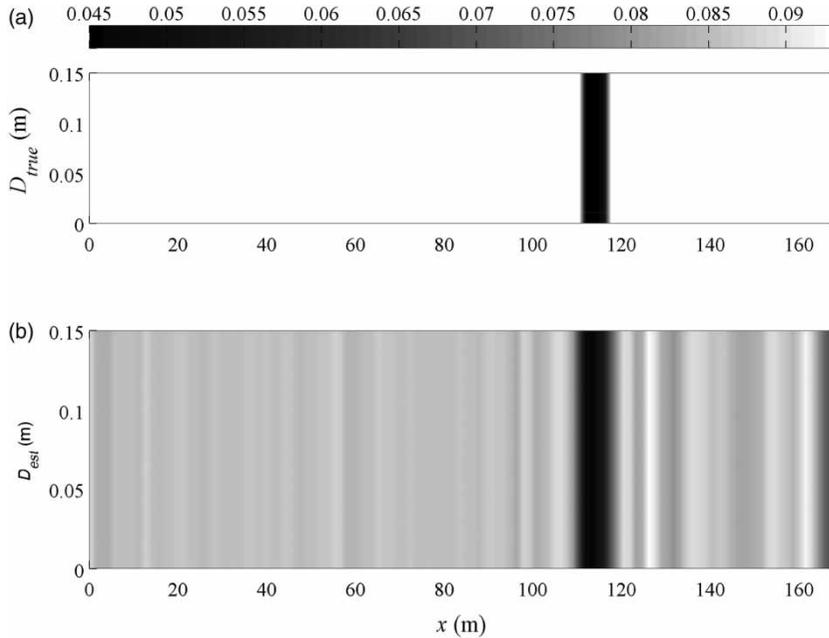
Figure 8 | Test 2: contour plot of the true (a) and the estimated diameters (b).

percentage errors Δ_D are plotted. The smaller diameters of pipe #2 are catched by inferring their reduction from location $x \cong 110$ m to location $x \cong 115$ m. The minimum value obtained for the diameter is 0.045 m with a relative percentage error with respect to the true diameter ($D_2 = 0.0383$ m) equal to 21%. Larger errors (of about 35%) shown in Figure 7(b) at pipe #2 section changes are due to the parameterization of the pipe system. From the measurement section to the location $x \cong 110$ m, the relative errors remain small spreading around $\Delta_D = 5\%$, while after location $x \cong 115$ m the error increases to a maximum value of 30%. Since the noise is not added to the signal, such errors are probably caused by model structure errors. In practice, when the signal is affected by noise or errors due to the model structure, in the pipe upstream of the partial blockage ($115 \text{ m} \leq x \leq 176.23 \text{ m}$) SLE shows a higher uncertainty of the estimates with respect to the downstream pipe.

A statistical analysis of Δ_D provides a mean value of 2.6×10^{-4} m and a standard deviation of ± 0.0632 m that is of the same order of magnitude of the diameter value. The MSE yields 4.5×10^{-3} m, about one order of magnitude smaller than the diameter value. In practice, SLE shows a good accuracy because it gives a good approximation of

the mean value of Δ_D, but with less precision, because of a relatively high standard deviation. A clear idea of such estimation results is given in a contour plot diagram where both actual and estimated diameters are reported (Figure 8); note that the darker the color, the smaller the diameter.

Furthermore, to figure out the uncertainty obtained in the estimation, Figure 9 shows the conditional variance of the diameters, which reflects the relative error path
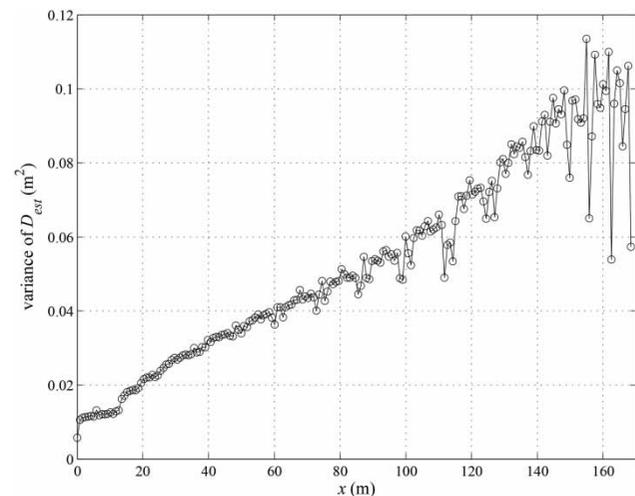

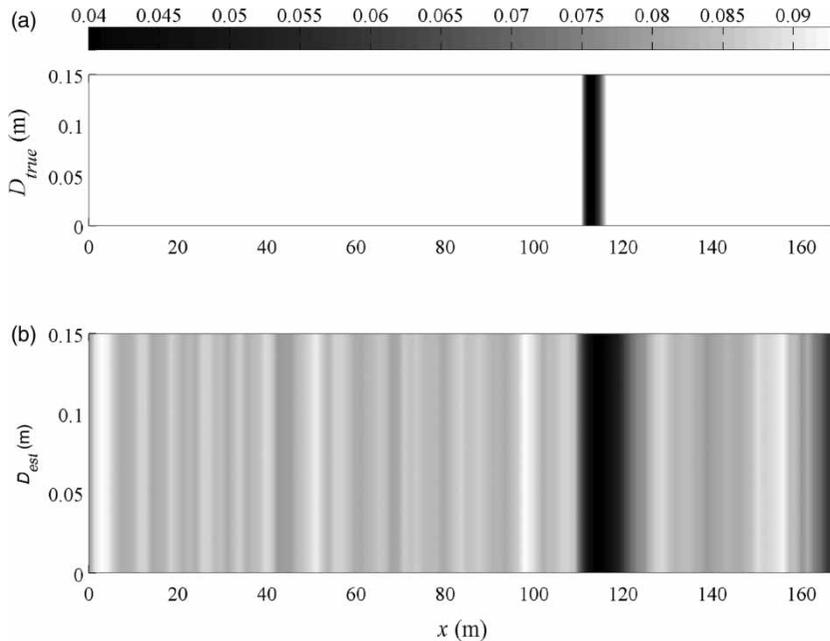**Figure 9** | Test 2: conditional variance of the estimated diameters.

Figure 10 │ Test 3: contour plot of the (a) true diameters and (b) estimated diameters vs. the location *x*.

increasing as it moves away from the measurement section.

Test 3

The pipe is discretized into 200 blocks as for test 2. To estimate the pipe diameters, SLE converges in 36 iterations with a computational time of almost 2 days (CPU Intel Core Duo 2.16 GHz, RAM 4 Gb). Figure 10 compares the contour plot of the true and the estimated diameters along the pipe. From the figure it can be seen that the pattern of the diameter distribution is satisfactorily detected although the estimation is less precise to infer diameter sharp variations. The latter is mainly due to the model structure errors and the simplicity of some assumptions such that of constant wave speed for all the pipes.

Figure 11 shows the behavior of Δ_D. It can be seen that the minimum value of Δ_D obtained for the diameters located at the blockage position is 23% corresponding to a diameter of 47.40 mm, whereas the maximum error is about 50% occurring close to the section changes. From location $x = 0$ to about $x = 110$ m the noise in the pressure signal reflects on the estimated diameters producing some oscillations of the estimates around the true value with relative errors
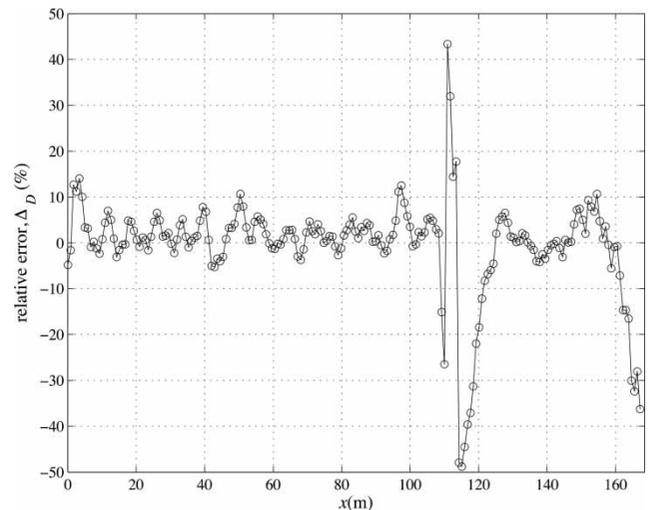

Figure 11 │ Test 3: relative percentage error Δ_D between estimated and true diameters along the location *x*.

spreading around 10% (about 1 cm). Upstream of the partial blockage the oscillation errors are larger, probably due to the inadequately modeled wave scattering between the blockage and the reservoir.

To have an idea of the capability of SLE in partial blockage positioning, as a first approximation, the extent and location associated with a given relative error in the
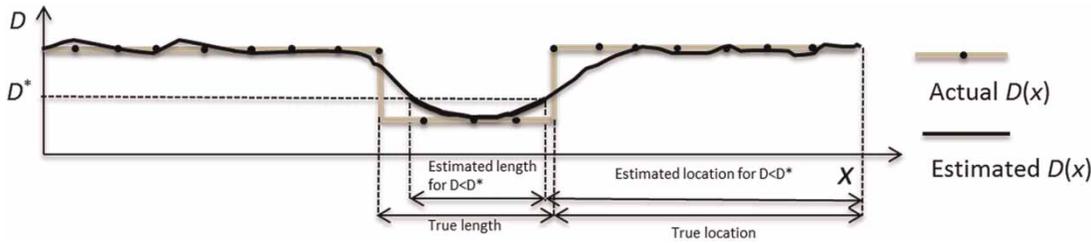
Figure 12 │ Test 3: schematization of blockage extent and location evaluation (D^* is the diameter associated with a given relative error in sizing).

diameter sizing can be determined (Figure 12 and Table 3). As an example, if the error in sizing is $\Delta_D = 30\%$ (corresponding to a diameter $D^* = 0.05$ m) the extent is $L_{2est} = 1.7$ m – which corresponds to a relative error (evaluated by Equation (14) with $f = L_2$) equal to $\Delta_{L2} = 48\%$ – and the location is $L_{1est} = 115.6$ m ($\Delta_{L1} = 4\%$). From Table 3 it can be seen that SLE provides good results to determine the location whereas less accurate results are obtained to infer the extent of the partial blockage.

Test 4

The pipe is discretized into 200 blocks leading to a spatial resolution $\Delta x = 0.8577$ m and a time step $\Delta t = 0.0023$ s. The pressure signal is downsampled by means of a linear interpolation, obtaining 440 head values. According to the parameterization, the blockage position is at $x = 110.6369$ m, equal to 129 blocks, and its extent is $L_2 = 6.86$ m, equal to eight blocks. As an initial guess for the estimation procedure, the pipe diameter $D = D_1$ is constant. In this case, SLE converges in 26 iterations with a computational time of almost 2 days (CPU Intel Core Duo 2.16 GHz, RAM 4 Gb).

Figure 13 shows the contour plot of the true and estimated diameters along x, while the relative percentage errors are displayed in Figure 14. Such results are very similar to the previous case with smooth variations of the

diameter distribution at cross-section changes (error up to 50%). However, in this case a better estimation of the blockage diameter is obtained with the smallest diameter $D = 0.0417$ m ($\Delta_D = 7.5\%$). Better results are also obtained in the blockage location, as can be seen in Table 4, with only 10% for $D^* < 0.05$ m. Such better results could be explained by the faster closure maneuver with respect to test 3.

CONCLUSIONS

In this paper the stochastic SLE, previously proposed in groundwater inverse problems, is used to locate and size partial blockages in pressurized pipes. Since SLE allows estimation of the diameter distribution, the diagnosis of pipe systems is cast in the probabilistic framework and the parameters are treated as stochastic processes.

To test SLE in the detection of partial blockages in viscoelastic pipes, numerical and laboratory tests are presented. With respect to previous papers, in the numerical experiments (tests 1a, 1b, and 2) the effect of an added noise and model parameters and structure is evaluated; laboratory tests allow the role played by unsteady friction and viscoelasticity to be pointed out.

On the basis of such experiments, it is shown that errors affecting the performance of SLE reflect mainly in the branches located at cross-section changes. In particular, a smooth variation of the diameter between the main pipe and the small-bore pipe simulating the partial blockage is observed.

The main sources of uncertainty are parameterization and model structure errors. For the first source, higher resolution and powerful calculators can help, whereas for the latter a more reliable model to simulate transients has to be adopted. A further source of uncertainty can be reduced by a correct filtering of the signal.

Table 3 │ Test 3: position and location of the partial blockage inferred by the diameter distribution with a given value of the diameter D^*

D^* (mm)	Δ_D (%)	L_{2est} (m)	Δ_{L2}	L_{1est} (m)	Δ_{L1}
50	30	1.70	48	115.6	4
60	50	5.95	44	113	2.7
70	80	6.80	51	113	2.7
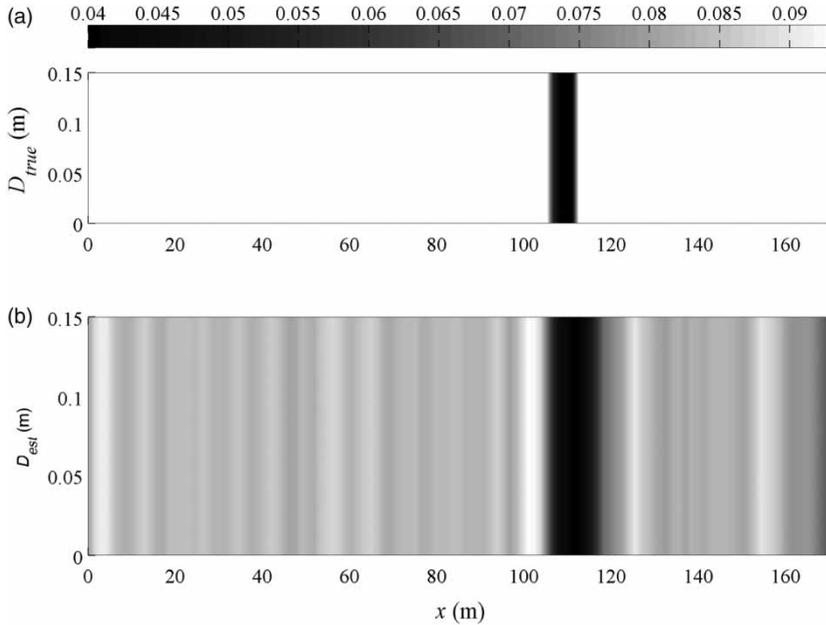
Figure 13 | Test 4: contour plot of the (a) true diameters and (b) estimated diameters vs. the location x.

Although the above issues still need to be assessed, it is shown that SLE can be used to detect extended partial blockages in simple pipelines and to approximate their size and location.
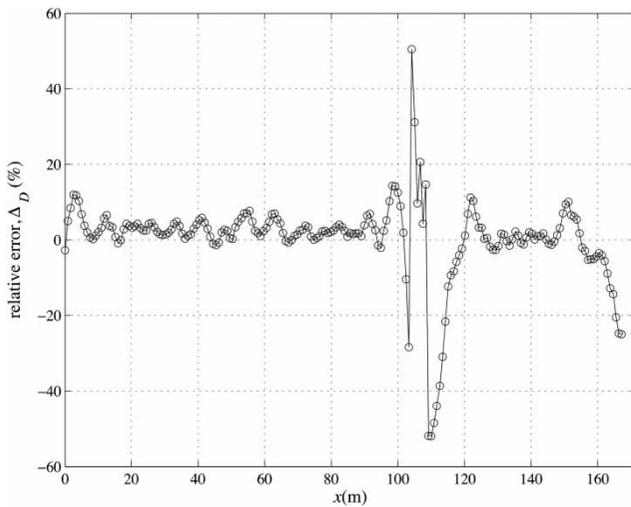

Figure 14 | Test 4: relative percentage error Δ_D between estimated and true diameters along the location x.

Table 4 | Test 4: position and location of the partial blockage inferred by the diameter distribution with a given value of the diameter D^*

D^* (mm)	Δ_D (%)	L_{2est} (m)	Δ_{L2}	L_{1est} (m)	Δ_{L1}
50	30	5.95	9.84	107.95	2.2
60	50	8.50	28.80	107.10	3
70	80	11.05	67	113.00	4.9

REFERENCES

Bergant, A., Simpson, A. & Vitkovsky, J. 2001 Developments in unsteady pipe flow friction modelling. *J. Hydraul. Res.* **39** (3), 249–257.

Boulos, P. F., Lansey, K. E. & Karney, B. W. 2006 *Comprehensive Water Distribution Systems Analysis Handbook for Engineers and Planners*, 2nd edn. MWH SOFT, Pasadena, CA.

Brunone, B. & Berni, A. 2010 Wall shear stress in transient turbulent pipe flow by local velocity measurement. *J. Hydraul. Eng.* **136** (10), 716–726.

Brunone, B. & Golia, U. M. 2008 Discussion of 'Systematic evaluation of one-dimensional unsteady friction models in simple pipelines' by J. P. Vitkovsky, A. Bergant, A. R. Simpson, and M. F. Lambert. *J. Hydraul. Eng.* **134** (2), 282–284.

Brunone, B., Golia, U. M. & Greco, M. 1995 Effects of two-dimensionality of pipes transients modeling. *J. Hydraul. Eng.* **121** (12), 906–912.

Brunone, B., Ferrante, M. & Meniconi, S. 2008 Discussion of 'Detection of partial blockage in single pipelines' by P. K. Mohapatra, M. H. Chaudhry, A. A. Kassem, and J. Moloo. *J. Hydraul. Eng.* **134** (6), 872–874.

Contractor, D. N. 1965 The reflection of waterhammer pressure waves from minor losses. *J. Basic Eng.* **87**, 445–451.

Covas, D., Stoianov, I., Mano, J., Ramos, H., Graham, N. & Maksimovic, C. 2005 The dynamic effect of pipe-wall viscoelasticity in hydraulic transients. Part II – model development, calibration and verification. *J. Hydraul. Res.* **43** (1), 56–70.

Dettinger, M. D. & Wilson, J. L. 1981 First order analysis of uncertainty in numerical models of groundwater flow part: 1. Mathematical development. *Water Resour. Res.* **17** (1), 149–161.

Duan, H.-F., Ghidaoui, S. M., Lee, J. P. & Tung, Y. K. 2010 Unsteady friction and viscoelasticity in pipe fluid transients. *J. Hydraul. Res.* **48** (3), 354–362.

Duan, H.-F., Lee, J. P., Ghidaoui, S. M. & Tung, Y. K. 2012a Extended blockage detection in pipelines by using the system frequency response analysis. *J. Water Resour. Plann. Manage.* **138** (1), 55–62.

Duan, H.-F., Ghidaoui, S. M., Lee, J. P. & Tung, Y. K. 2012b Relevance of unsteady friction to pipe size and length in pipe fluid transients. *J. Hydraul. Eng.* **138** (2), 154–166.

Duan, H., Lee, P., Kashima, A., Lu, J., Ghidaoui, M. & Tung, Y. 2013 Extended blockage detection in pipes using the system frequency response: analytical analysis and experimental verification. *J. Hydraul. Eng.* **139** (7), 763–771.

Duan, H., Lee, P., Ghidaoui, M. & Tuck, J. 2014a Transient wave-blockage interaction and extended blockage detection in elastic water pipelines. *J. Fluids Struct.* **46**, 2–16.

Duan, H., Lee, P. & Ghidaoui, M. 2014b Transient wave-blockage interaction in pressurized water pipelines. In: *Proceedings of the 12th International Conference on Computing and Control for the Water Industry – CCWI2013*. Procedia Engineering, Elsevier, Perugia, 70, pp. 573–582.

Ferrante, M., Brunone, B. & Meniconi, S. 2007 Wavelets for the analysis of transient pressure signals for leak detection. *J. Hydraul. Eng.* **133** (11), 1274–1282.

Ferrante, M., Brunone, B. & Meniconi, S. 2009a Leak detection in branched pipe systems coupling wavelet analysis and a Lagrangian model. *J. Water Supply Res. Technol. AQUA* **58** (2), 95–106.

Ferrante, M., Brunone, B. & Meniconi, S. 2009b Leak-edge detection, *J. Hydraul. Res.* **47** (2), 233–241.

Franke, P. & Seyler, F. 1983 Computation of unsteady pipe flow with respect to visco-elastic material properties. *J. Hydraul. Res.* **21** (5), 345–353.

Keramat, A., Tijsseling, A. S., Hou, Q. & Ahmadi, A. 2012 Fluid–structure interaction with pipe-wall viscoelasticity during waterhammer. *J. Fluids Struct.* **28**, 434–455.

Kitanidis, P. K. & Vomvoris, E. G. 1983 A geostatistical approach to the inverse problem in groundwater modeling (steady state) and one-dimensional simulations. *Water Resour. Res.* **19** (3), 677–690.

Lee, P. J., Vitkovsky, J. P., Lambert, M. F., Simpson, A. R. & Liggett, J. A. 2008 Discrete blockage detection in pipelines using the frequency response diagram: numerical study. *J. Hydraul. Eng.* **134** (5), 658–663.

Lee, P., Duan, H., Ghidaoui, M. & Karney, B. 2013 Frequency domain analysis of pipe fluid transient behaviour. *J. Hydraul. Res.* **51** (6), 609–622.

Liggett, J. A. & Chen, L. C. 1994 Inverse transient analysis in pipe networks. *J. Hydraul. Eng.* **120** (8), 934–955.

Massari, C., Yeh, T.-C. J., Ferrante, M., Brunone, B. & Meniconi, S. 2013a Diagnosis of pipe systems by means of a stochastic successive linear estimator. *Water Resour. Manage.* **27** (13), 4637–4654.

Massari, C., Yeh, T.-C. J., Ferrante, M., Brunone, B. & Meniconi, S. 2013b Diagnosis of pipe systems by the SLE: first results. *J. Water Supply Res. Technol. AQUA* **13** (4), 958–965.

Massari, C., Yeh, T.-C. J., Ferrante, M., Brunone, B. & Meniconi, S. 2014a Detection and sizing of extended partial blockages in pipelines by means of a stochastic successive linear estimator. *J. Hydroinform.* **16** (2), 248–258.

Massari, C., Yeh, T.-C. J., Ferrante, M., Brunone, B. & Meniconi, S. 2014b A stochastic tool for determining the presence of partial blockages in viscoelastic pipelines: first experimental results. In: *Proceedings of the 12th International Conference on Computing and Control for the Water Industry – CCWI2013*. Procedia Engineering, Elsevier, Perugia, 70, pp. 1112–1120.

Meniconi, S., Brunone, B., Ferrante, M. & Massari, C. 2010 Potential of transient tests to diagnose real supply pipe systems: what can be done with a single extemporary test. *J. Water Resour. Plann. Manage.* **137** (2), 238–241.

Meniconi, S., Brunone, B. & Ferrante, M. 2011a In-line pipe device checking by short-period analysis of transient tests. *J. Hydraul. Eng.* **137** (7), 713–722.

Meniconi, S., Brunone, B., Ferrante, M. & Massari, C. 2011b Small amplitude sharp pressure waves to diagnose pipe systems. *Water Resour. Manage.* **25** (1), 79–96.

Meniconi, S., Brunone, B. & Ferrante, M. 2012a Water-hammer pressure waves interaction at cross-section changes in series in viscoelastic pipes. *J. Fluids Struct.* **33**, 44–58.

Meniconi, S., Brunone, B., Ferrante, M. & Massari, C. 2012b Transient hydrodynamics of in-line valves in viscoelastic

pressurized pipes: long-period analysis. *Exp. Fluids* **53** (1), 265–275.

Meniconi, S., Duan, H.-F., Lee, P. J., Brunone, B., Ghidaoui, M. & Ferrante, M. 2013 Experimental investigation of coupled frequency- and time-domain transient test-based techniques for partial blockage detection in pipelines. *J. Hydraul. Eng.* **139** (10), 1033–1040.

Meniconi, S., Brunone, B., Ferrante, M. & Massari, C. 2014 Energy dissipation and pressure decay during transients in viscoelastic pipes with an in-line valve. *J. Fluids Struct.* **45**, 235–249.

Mohapatra, P. K., Chaudhry, M. H., Kassem, A. A. & Moloo, J. 2006a Detection of partial blockage in single pipelines. *J. Hydraul. Eng.* **132** (2), 200–206.

Mohapatra, P. K., Chaudhry, M. H., Kassem, A. A. & Moloo, J. 2006b Detection of partial blockages in a branched piping system by the frequency response method. *J. Fluids Eng.* **128** (5), 1106–1114.

Papadopoulou, K. A., Shamout, M. N., Lennox, B., Mackay, D., Taylor, A. R., Turner, J. T. & Wang, X. 2008 An evaluation of acoustic reflectometry for leakage and blockage detection. *Proc. IMechE, Part C J. Mech. Eng. Sci.* **222**, 959–966.

Pezzinga, G. 2000 Evaluation of unsteady flow resistances by quasi-2D or 1D models. *J. Hydraul. Eng.* **126** (10), 778–785.

Pezzinga, G., Brunone, B., Cannizzaro, D., Ferrante, M., Meniconi, S. & Berni, A. 2014 Two-dimensional features of viscoelastic models of pipe transients. *J. Hydraul. Eng.* **140** (8), 04014036.

Sattar, A. M., Chaudhry, M. H. & Kassem, A. A. 2008 Partial blockage detection in pipelines by frequency response method. *J. Hydraul. Eng.* **134** (1), 76–89.

Soares, A., Covas, D. & Reis, L. 2008 Analysis of PVC pipe-wall viscoelasticity during water hammer. *J. Hydraul. Eng.* **134** (9), 1389–1395.

Stephens, M. L., Lambert, M. F., Simpson, A. R., Vitkovsky, J. P. & Nixon, J. B. 2004 Field test for leakage, air pocket and discrete blockage detection using inverse transient analysis in water distribution pipes. In: *Proceedings of the 2004 World Water and Environmental Research Congress.* ASCE, 27 June–1 July 2004, Salt Lake City, UT (G. Sehlke, D. F. Hayes & D. K. Stevens, eds). pp. 1–10.

Tuck, J., Lee, P., Davidson, M. & Ghidaoui, M. 2013 Analysis of transient signals in simple pipeline systems with an extended blockage. *J. Hydraul. Res.* **51** (6), 623–633.

Vargas-Guzmán, J. A. & Yeh, T.-C. J. 2002 The successive linear estimator: a revisit. *Adv. Water Resour.* **25** (7), 773–781.

Wang, X.-J., Lambert, M. & Simpson, A. 2005 Detection and location of a partial blockage in a pipeline using damping of fluid transients. *J. Water Resour. Plann. Manage.* **131** (3), 244–249.

Yeh, T.-C. J. & Zhang, J. 1996 A geostatistical inverse method for variably saturated flow in the vadose zone. *Water Resour. Res.* **32** (9), 2757–2766.

Yeh, T.-C. J., Jin, M. & Hanna, S. 1996 An iterative stochastic inverse method: conditional effective transmissivity and hydraulic head fields. *Water Resour. Res.* **32** (1), 85–92.

Zhu, J. & Yeh, T.-C. J. 2005 Characterization of aquifer heterogeneity using transient hydraulic tomography. *Water Resour. Res.* **41** (7), W07028.